

Tachyon inflation in theory with non-minimal matter-curvature coupling

Abolhassan Mohammadi* and Fardin Kheirandish
*Department of Physics, Faculty of Science, University of Kurdistan,
Pasdaran Street, P.O. Box 66177, Sanandaj, Iran.*

(Dated: February 13, 2023)

In this study, we explore the phenomenon of tachyon inflation in the context of the alternative gravity theory $f(R, T)$, which includes a non-minimal coupling between matter and curvature. By applying slow-roll approximations, we examine the model in detail for three different potentials: power-law, generalized T-mode, and inverse hyperbolic cosh. Using observational data and Python coding, we determine a range of values for the model's free parameters that allow it to fit the data perfectly. In essence, this study provides a comprehensive analysis of tachyon inflation in the $f(R, T)$ gravity theory, offering new insights into this alternative framework and its potential to explain tachyon inflation.

PACS numbers: 04.50.Kd, 04.20.Cv, 04.20.Fy

Keywords: $f(R, T)$ gravity, inflation, tachyon field, slow-roll approximations.

I. INTRODUCTION

The search for solution to the problems of the hot Big Bang Theory, led to the introduction of the inflationary scenario. The scenario states that the universe in the earliest phase undergoes an extreme expansion in a short period of time. After its first proposal [1–5], the scenario has been modified and developed in different ways and in various frame of gravity theories [6–45]. A common perspective is that inflation is driven by a scalar field, which is the dominant component of the universe at the time. It stands on top of the potential, and slowly rolls down toward the minimum of the potential. During this slowly rolling, the potential does not change dramatically and a quasi-de Sitter expansion is produced [46–54]. The scalar field which governs inflation is called inflaton and there are different candidates for it such as canonical scalar field, tachyon field, and DBI field. The scenario of inflation has received tremendous support by the data [55–57] and become the cornerstone of any cosmological model.

Einstein's theory of general relativity is the most well-known and accepted theory of gravity, proposed in 1915. The theory explains how objects are affected by gravity, and it also explains how light bends when passing near a massive object. Einstein's theory of general relativity has been tested many times to see if it would work or not. Besides all the success of the Einstein's theory of gravity, there have been serious attempt for introducing alternative theories of gravity [58–66]. The main motivation for all this effort is that general relativity is unable to fit the cosmological data without including dark energy and dark matter. One of these alternative theories, which we will focus on, is $f(R, T)$ theory of gravity. The theory contains a non-minimal coupling between the matter sector and the curvature. The theory was first proposed by Harko et. al. [67] and since then has been used for studying different astrophysical and cosmological topics [68–75]; including inflation [76–79].

Most of the work on inflation in $f(R, T)$ gravity theory concentrated on applying a canonical scalar field for the role of inflaton, and there are no attempts to consider other candidates such as tachyon field (refer to [80] for a review on tachyon field). Tachyon inflation is a type of inflationary cosmology that has gained attention as a possible explanation for the early universe's rapid expansion. Tachyon inflation in Einstein's gravity has been studied extensively, and the result showed also a great consistency with the data. In $f(R, T)$ gravity theory, the action for the gravitational field is modified to include a non-minimal coupling between curvature and matter, represented by the "T" term. This results in a different evolution of the universe compared to standard inflationary models. In the current paper, we are going to consider the scenario of slow-roll tachyon inflation in the frame of $f(R, T)$ gravity theory. During this specific time, the potential energy density of the field plays the main role, and we consider the model for different types of the potential.

The paper is organized as follows: there is a general and brief look on the theory of $f(R, T)$ gravity in Sec.II. Next, The tachyon field is introduced in Sec.III, which plays the role of inflaton. The field energy density and pressure

* a.mohammadi@uok.ac.ir; abolhassanm@gmail.com

are inserted in the Friedmann equation, and they will be simplified by applying the slow-roll approximations. The perturbation parameters are introduced, which play important role for comparing the model with the data. Then, in Sec.IV, the model is considered in detail for three types of the potential and the free parameters of the model are determined by performing a coding programming. Finally, the results are summarized in Sec.V.

II. BASIC EQUATIONS IN $f(R, T)$ GRAVITY

In a general shape, the action of the $f(R, T)$ theory of gravity is assumed to be given as follows [67]

$$S = \frac{1}{2\kappa^2} \int d^4x \sqrt{-g} \left(f(R, T) + \mathcal{L}_m \right) \quad (1)$$

in which R is known as the curvature scalar and T stands for the trace of the energy-momentum tensor. $f(R, T)$ is an arbitrary function of curvature scalar R and the trace T . The determinant of the spacetime metric $g_{\mu\nu}$ is indicated by g . The Lagrangian density for the matter sector is described by \mathcal{L}_m . The gravitational constant is given through the quantity κ as $\kappa^2 = 8\pi G$.

The field equations of the theory is achieved by taking variation of the action with respect to the metric $g_{\mu\nu}$, which leads to the following Friedmann equations after substituting the spatially flat FLRW metric [76]

$$H^2 = \frac{\kappa^2}{3} \left(\left(\frac{3}{2}\lambda + 1 \right) \rho - \frac{\lambda}{2} p \right), \quad (2)$$

$$-3H^2 - 2\dot{H} = \kappa^2 \left(-\frac{\lambda}{2} \rho + \left(\frac{3}{2}\lambda + 1 \right) p \right), \quad (3)$$

where $f(R, T)$ is picked out as $f(R, T) = R + \eta T$, with constant $\eta = \lambda\kappa^2$. This choice for $f(R, T)$ is utilized for studying different cosmological topics [67, 81–89]. Moreover, the energy-momentum tensor is assumed to be described by a perfect fluid with a diagonal shape $T_\nu^\mu = \text{diag}(\rho, -p, -p, -p)$, in which ρ and p respectively stands for the energy density and pressure of the matter field.

Taking the Hubble parameter from Eq.(2) and inserting it in Eq.(3), one arrives at

$$-2\dot{H} = \kappa^2 (1 + \lambda) (\rho + p). \quad (4)$$

Due to the non-minimal interaction between the matter and the curvature, the conservation equation is modified. Here, the equation could be obtained from Eqs.(2) and Eq.(4) by taking the time derivative from the first one and inserting the second. The resulted relation is

$$\dot{\rho} + 3H (\rho + p) = -\frac{3\lambda}{2} \dot{\rho} + \frac{\lambda}{2} \dot{p} - 3\lambda H (\rho + p) \quad (5)$$

where the terms of the right-hand side of the equation are the modified terms compared to the standard one. All above equations return to the standard ones by imposing $\lambda = 0$.

III. TACHYON INFLATION

Inflation is assumed to be governed by tachyon field with the following action

$$\mathcal{L} = -V(\phi) \sqrt{1 - \dot{\phi}^2}, \quad (6)$$

where ϕ stands for the tachyon field and $V(\phi)$ is the potential of the tachyon field. The corresponding energy density and pressure are read as

$$\rho = \frac{V(\phi)}{\sqrt{1 - \dot{\phi}^2}}, \quad p = -V(\phi) \sqrt{1 - \dot{\phi}^2}. \quad (7)$$

Inserting above energy density and pressure in Eq.(2), one arrives at

$$H^2 = \frac{\kappa^2}{3} \frac{V(\phi)}{\sqrt{1 - \dot{\phi}^2}} \left((2\lambda + 1) - \frac{\lambda}{2} \dot{\phi}^2 \right). \quad (8)$$

Also, by substituting Eq.(7) in Eq.(4) and using the Friedmann equation (8), we have

$$\frac{-\dot{H}}{H^2} = \frac{3}{2} \frac{(1+\lambda)\dot{\phi}^2}{(2\lambda+1) - \frac{\lambda}{2}\dot{\phi}^2}. \quad (9)$$

The term on the right-hand side of the above equation is known as the definition of the first slow-roll parameter. The first slow-roll approximation states that the rate of the Hubble parameter during a Hubble time is smaller than unity

$$\epsilon_1 \equiv \frac{-\dot{H}}{H^2} \ll 1. \quad (10)$$

It leads to this conclusion that the time derivative of the field should be much smaller than one, i.e. $\dot{\phi}^2 \ll 1$. On the other hand, the field equation of motion is achieved from Eqs.(5) and (7)

$$\left(\frac{\frac{3\lambda}{2} + 1}{1 - \dot{\phi}^2}\right) \ddot{\phi} + 3(1+\lambda)H\dot{\phi} + \left(\left(\frac{3\lambda}{2} + 1\right) + \frac{\lambda(1 - \dot{\phi}^2)}{2}\right) \frac{V'}{V} = 0, \quad (11)$$

where prime indicates derivative with respect to the tachyon field.

Another slow-roll parameter is defined through the time derivatives of the field. It states that the rate of $\dot{\phi}$ during a Hubble time is smaller than one, i.e.

$$\delta = \frac{\ddot{\phi}}{H\dot{\phi}} \ll 1. \quad (12)$$

A. Equations under slow-roll approximations

After applying the slow-roll approximations, the dynamical equations of the model gain a more simple form and are rewritten as

$$H^2 = \frac{\kappa^2}{3} (2\lambda + 1) V(\phi), \quad (13)$$

$$\dot{H} = \frac{-\kappa^2}{2} (1 + \lambda) \dot{\phi}^2 V(\phi), \quad (14)$$

$$3H\dot{\phi} = -\frac{2\lambda + 1}{\lambda + 1} \frac{V'}{V}. \quad (15)$$

From Eqs.(13) and (11), the time derivative of the tachyon field is obtained as

$$\dot{\phi}^2 = \frac{1}{\kappa^2} \frac{2\lambda + 1}{(\lambda + 1)^2} \frac{V'^2}{V^3}. \quad (16)$$

The above equations are utilized to express the slow-roll parameter ϵ_1 in terms of the potential

$$\epsilon_1 = \frac{3}{2\kappa^2} \frac{1}{(1+\lambda)} \frac{V'^2}{V^3} = \frac{3}{2} \frac{(1+\lambda)}{(1+2\lambda)} \dot{\phi}^2. \quad (17)$$

Besides the second slow-roll parameter δ which introduced in Eq.(12) and commonly used, there is a well-known hierarchy procedure for defining the slow-roll parameters as

$$\epsilon_{n+1} = \frac{\dot{\epsilon}_n}{H\epsilon_n}, \quad n \geq 1. \quad (18)$$

Defining the slow-roll parameter through this procedure would be more efficient for us when we are going to work with the perturbation parameters. The second slow-roll parameter ϵ_2 is derived as¹

$$\epsilon_2 = \frac{\dot{\epsilon}_1}{H\epsilon_1} = \frac{1}{\kappa^2(1+\lambda)} \left(\frac{3V'^2}{V^3} - 2\frac{V''}{V^2} \right). \quad (19)$$

¹ Note that for this model, the slow-roll parameter ϵ_2 is very close to the slow-roll parameter δ ; namely $\epsilon_2 = 2\ddot{\phi}/H\dot{\phi} = 2\delta$.

B. Perturbations

Quantum fluctuations refer to the tiny fluctuations in the density of the universe that arise due to the uncertainty principle of quantum mechanics. In the inflationary scenario of the universe, these fluctuations are thought to be the seeds of all structure in the universe, including galaxies, clusters, and superclusters. During inflation, the universe is thought to have undergone a rapid expansion, stretching quantum fluctuations in the matter and energy density to macroscopic scales. These fluctuations were then frozen into the fabric of spacetime and served as the initial conditions for the formation of structure in the universe. This scenario is supported by several observational evidences, such as the cosmic microwave background radiation, which shows fluctuations in temperature that match the predictions of inflationary models. Overall, quantum fluctuations in the inflationary scenario of the universe play a crucial role in the formation of structure in the universe and have been confirmed by various observations, making them an important aspect of our understanding of the early universe and the evolution of the cosmos.

For any new inflationary model, it is vital to be checked with the data. In this regard, we introduce the essential perturbation parameters for our model here, and then we are going to use them in the next section where the model is being compared with data for different types of the potentials. Regarding scalar perturbations, we have the amplitude of the scalar perturbations which is read as [90]²

$$\mathcal{P}_s = \frac{1}{4\pi^2} \frac{H^4}{c_s(\rho_{eff} + p_{eff})} \quad (20)$$

where c_s is the sound speed, defined as³

$$c_s^2 = \frac{\dot{p}_{eff}}{\dot{\rho}_{eff}} = \frac{(1 + \lambda) - (1 + \frac{3}{2}\lambda) \dot{\phi}^2}{(1 + \lambda) + \frac{1}{2}\lambda \dot{\phi}^2}, \quad (21)$$

and

$$\begin{aligned} \rho_{eff} &= \left(\left(\frac{3}{2}\lambda + 1 \right) \rho - \frac{\lambda}{2} p \right) \\ p_{eff} &= \left(-\frac{\lambda}{2} \rho + \left(\frac{3}{2}\lambda + 1 \right) p \right) \end{aligned}$$

with ρ and p are the energy density and pressure of tachyon field given by Eq.(7).

The scalar spectral index, which is defined through the amplitude of the scalar field, is given by

$$n_s = 1 - (2\epsilon_1 + \epsilon_2 + s). \quad (22)$$

where $s = \dot{c}_s/Hc_s$ is another slow-roll parameter which determines the rate of the sound speed in a Hubble time. Regarding the tensor perturbations, there is the tensor-to-scalar ratio, which is very essential in examining an inflationary model. The parameter is expressed as follows

$$r = 16 c_s \epsilon_1. \quad (23)$$

In the following section, we are going to examine the model for some specific types of the potential and compare the results with data.

IV. TYPICAL EXAMPLES

In this section, three types of potentials as power-law, generalized T-mode, and the inverse coshyperbolic are taken, and the model is studied in detail for each case.

² From [90] and the shape of the action (1) and (6), it is realized that the effective matter Lagrangian could in general be written as a function of $X = \dot{\phi}^2/2$ and the potential $V(\phi)$, in another word, the lagrangian density of the matter field is $\mathcal{L}(\phi, X)$. Then, the model is a k-essence model and the quantum perturbations of the k-essence model is studied in [90].

³ In general, the sound speed is defined as $c_s^2 = \dot{p}/\dot{\rho}$. But, in our case, the energy density and pressure in the relation are not the energy density and pressure defined through Eq.(7). In fact, they are the effective energy density and pressure which is defined from the right-hand side of Eqs.(2) and (3).

A. power-law

We begin with the most common potential, i.e. power-law potential

$$V(\phi) = V_0 \phi^n. \quad (24)$$

Utilizing the potential, the first and second slow-roll parameters are obtained as

$$\epsilon_1 = \frac{3n^2}{2\kappa^2(1+\lambda)V_0} \frac{1}{\phi^{n+2}}, \quad (25)$$

$$\epsilon_2 = \frac{n(n+2)}{2\kappa^2(1+\lambda)V_0} \frac{1}{\phi^{n+2}}. \quad (26)$$

and the time derivative of the scalar field is derived by inserting the potential (24) in (14) as

$$\dot{\phi}^2 = \frac{n^2(1+2\lambda)}{2\kappa^2(1+\lambda)^2V_0} \frac{1}{\phi^{n+2}} \quad (27)$$

Inflation ends as the acceleration reaches zero, which is expressed by the relation $\epsilon_1 = 1$. Solving the relation, one can estimate the scalar field value at the end of inflation as

$$\phi_e^{n+2} = \frac{3n^2}{2\kappa^2(1+\lambda)V_0}. \quad (28)$$

Following the definition of the number of e-folds

$$N = \int_{t_*}^{t_e} H dt = \int_{\phi_*}^{\phi_e} \frac{H}{\dot{\phi}} d\phi \quad (29)$$

$$= -\kappa^2(1+\lambda) \int_{\phi_*}^{\phi_e} \frac{V^2}{V'} d\phi \quad (30)$$

and solving the integral, the scalar field is written as a function of the number of e-fold as

$$\phi_*^{n+2} = \frac{3n^2}{2\kappa^2(1+\lambda)V_0} \left(1 + \frac{2}{3} \frac{n+2}{n} N \right). \quad (31)$$

Using the potential and the obtained ϕ_* , and substituting them in the slow-roll parameters (17) and (19), the scalar spectral index and the tensor-to-scalar ratio are achieved

$$n_s = 1 - \frac{5n+2}{3n} \left(1 + \frac{2(n+2)}{3n} N \right)^{-1} \quad (32)$$

$$r = 16 \left(1 + \frac{2(n+2)}{3n} N \right)^{-1} c_s, \quad (33)$$

where the sound speed is obtained by combining Eqs.(21) and (27), and (31).

The perturbation parameters n_s and r depend on the model parameters n λ and the number of e-folds N . To solve the problems of hot Big Bang Theory, inflation is required to last for about 55-65 number of e-folds. Fig.1 illustrates $r - n_s$ diagram of the model in terms of the parameter n for different values of λ . It is seen that the results are in good agreement with observational data. The arrow in the figure displays the direction of the enhancement of the parameter n . By increasing of n , the tensor-to-scalar ratio increase, however the scalar spectral index gets smaller values.

Fig.2 portrays the parameter space of the model. The color region is a set of all (λ, n) points that drags the model predictions concerning n_s and r along with data. One find s that to provide the consistency with data, the parameter n should be positive and smaller than 0.28, however, the parameter λ takes a very wide range. Table.I expresses some of the n_s and r results for different values of n and λ that are picked from Fig.2. It shows that for the selected points (n, λ) , the scalar spectral index and the tensor-to-scalar ratio stand in the range provided by Planck [57]. Besides, the table presents the energy scale of inflation for the case. It states that the energy scale of inflation is of the order of $\mathcal{O}(10^{-3})(\text{GeV})$, below the Planck scale (note that the result is provided by taking $\kappa = 1$).

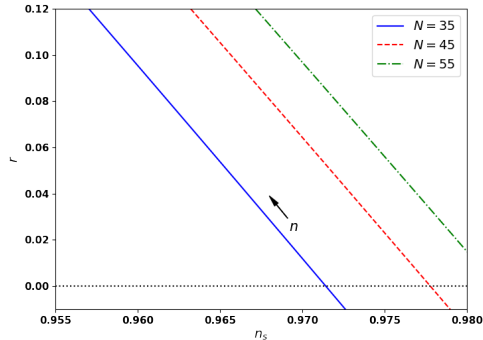


FIG. 1. The plot shows the $r - n_s$ diagram of the model in terms of the parameter n for different values of λ .

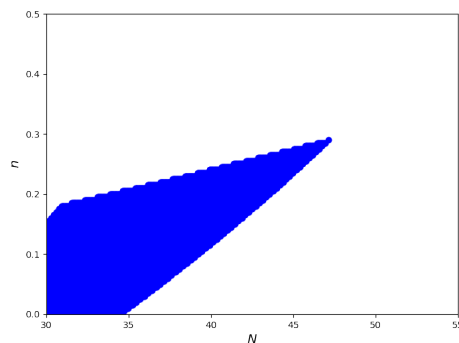


FIG. 2. The parameter space of the model for number of e-folds $N = 65$.

The other free parameter of the model, V_0 , is determined through the amplitude of the scalar perturbations, i.e. Eq.(20). Using Eqs.(13), (24), (25), and (31), the free parameter V_0 is obtained as

$$V_0 = \left[\frac{24\pi^2 c_s \epsilon_1 \mathcal{P}_s}{\kappa^2 (1 + 2\lambda)} \left(\frac{2\kappa^2 (1 + \lambda) \epsilon_1}{3n^2} \right)^{\frac{n}{n+2}} \right]^{\frac{n+2}{2}} \quad (34)$$

Table.I shows the numerical result for the constant V_0 for different values of n and λ . The magnitude of the

λ	n	N	n_s	r	V_0	ES
1.0	0.1	35	0.9675	0.0325	1.05×10^{-10}	4.28×10^{-3}
1.0	0.1	40	0.9715	0.0285	9.12×10^{-11}	4.14×10^{-3}
1.0	0.2	35	0.9639	0.0619	6.26×10^{-11}	5.03×10^{-3}
1.0	0.2	40	0.9684	0.0542	5.34×10^{-11}	4.86×10^{-3}
10^2	0.1	35	0.9676	0.0325	1.55×10^{-12}	1.50×10^{-3}
10^2	0.1	40	0.9716	0.0285	1.34×10^{-12}	1.45×10^{-3}
10^2	0.2	35	0.9641	0.0618	9.06×10^{-13}	1.76×10^{-3}
10^2	0.2	40	0.9685	0.0541	7.73×10^{-13}	1.70×10^{-3}
10^4	0.1	35	0.9676	0.0325	1.55×10^{-14}	4.74×10^{-4}
10^4	0.1	40	0.9716	0.0285	1.34×10^{-14}	4.58×10^{-4}
10^4	0.2	35	0.9641	0.0618	9.10×10^{-15}	5.56×10^{-4}
10^4	0.2	40	0.9685	0.0541	7.76×10^{-15}	5.38×10^{-4}

TABLE I. The table displays the numerical results of the model for different values of the parameters n and λ that are selected from parameter space Fig.2.

constant is of the order of $\mathcal{O}(10^{-10}$ to $10^{-15})$ depending mainly on the value of the parameter λ .

B. Generalized T-mode

For the second case, we are investigating a generalized T-mode potential

$$V(\phi) = V_0 \left(1 - \tanh^2(\alpha\phi)\right). \quad (35)$$

Inserting the potential in Eqs.(17) and (19), the slow-roll parameters are acquired as

$$\begin{aligned} \epsilon_1 &= \frac{6\alpha^2}{\kappa^2(1+\lambda)V_0} \frac{\tanh^2(\alpha\phi)}{1 - \tanh^2(\alpha\phi)}, \\ \epsilon_2 &= \frac{4\alpha^2}{\kappa^2(1+\lambda)V_0} \frac{1}{\tanh^2(\alpha\phi)} \end{aligned} \quad (36)$$

and $\dot{\phi}$ is read from Eq.(16)

$$\dot{\phi}^2 = \frac{4\alpha^2(1+2\lambda)}{\kappa^2(1+\lambda)^2V_0} \frac{\tanh^2(\alpha\phi)}{1 - \tanh^2(\alpha\phi)} \quad (37)$$

To estimate the scalar field at the end of inflation, it is required to solve the relation $\epsilon_1 = 1$. This lead to a second order equation, and the solution is given by

$$\tanh^2(\alpha\phi_e) = \frac{\beta}{1+\beta} \quad (38)$$

where the defined constant β is

$$\beta \equiv \frac{\kappa^2(1+\lambda)V_0}{6\alpha^2}.$$

By integrating the e-folds equation and after doing some manipulation, the scalar field at horizon crossing is derived

$$\tanh^2(\alpha\phi_*) = \frac{\beta}{1+\beta} \exp\left(\frac{-2N}{3\beta}\right). \quad (39)$$

Substituting the above result in the slow-roll parameters (36) and apply it into Eqs.(IIIB) and (23), the scalar spectral index and the tensor-to-scalar ratio are obtained in terms of the free parameters β , λ and the e-fold N .

$$n_s = 1 - \frac{2(1+\beta) + 6\beta e^{-2N/3\beta}}{3\beta\left((1+\beta) - \beta e^{-2N/3\beta}\right)} \quad (40)$$

$$r = 16 c_s \frac{e^{-2N/3\beta}}{(1+\beta) - \beta e^{-2N/3\beta}}, \quad (41)$$

where the sound speed at horizon crossing is read from Eqs.(21), (37), and (39).

The model predictions about scalar spectral index and the tensor-to-scalar is plotted in Fig.3, where r is plotted versus n_s for different values of parameter λ and the number of e-folds N . The variable parameter for $r - n_s$ curves is the parameter β which increase in the direction of the arrow. It is realized that the predictions could agree with data for the number of e-folds $N \geq 80$. For less number of e-folds, the values of the scalar spectral index stands outside the observational range, although the value of r remain below $r < 0.064$. Therefore, for the model to agree with the data it requires at least about 80 number of e-folds.

Fig.4 illustrates a range for the parameter β and the number of e-folds N to construct the model consistent with data. The color region are obtained via a python coding and by imposing the observational data about n_s and r on the model, i.e. Eqs.(40) and (41) which are obtained via a Python coding and using observational data. For $N = 80$, there is a narrow range for β . However, by increasing the number of e-folds, a wider range for the parameter β is provided. On the other hand, it is not our interest to have a high number of e-folds.

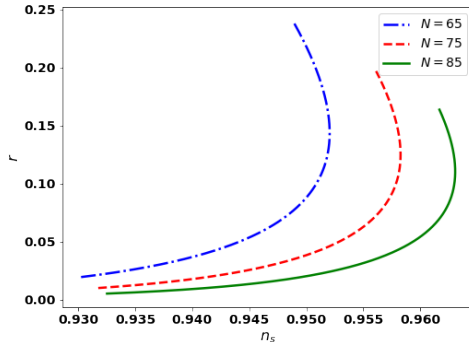


FIG. 3. The tensor-to-scalar ratio is plotted versus the scalar spectral index for different values of the parameter λ and the number of e-folds N . The variable parameter here is β and the arrow shows the direction of the enhancement of β .

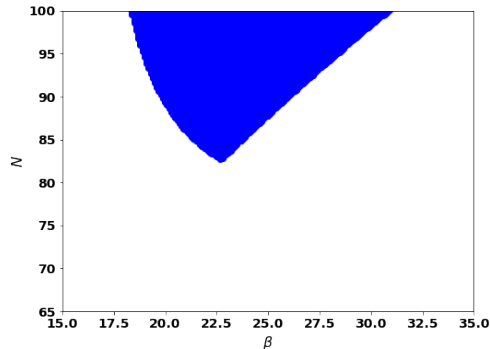


FIG. 4. The figure shows the parameter space for the model. The color region is a set of all (β, N) which put the model prediction about n_s and r in agreement with data.

Applying the potential on the Friedmann equation (13) and substituting it into the relation of the amplitude of the scalar field (20), the model free parameter V_0 is expressed as

$$V_0 = \frac{24\pi^2 c_s \epsilon_1 \mathcal{P}_s}{\kappa^2(1+2\lambda)(1-\tanh^2(\alpha\phi))} \quad (42)$$

Using data for \mathcal{P}_s and evaluating the above relation at the time of horizon crossing, the free parameter V_0 is determined. Table.(II) describes the result of the case in brief. It is seen that the constant should be of the order of $\mathcal{O}(10^{-10})$. Also, after determining β and V_0 , the constant α could easily be estimated from the definition of β . The constant α is of the order of $\mathcal{O}(10^{-6})$.

C. Inverse coshyperbolic potential

As the last case, we consider the inverse coshyperbolic potential [91–94], given by

$$V(\phi) = \frac{V_0}{\cosh(\alpha\phi)}. \quad (43)$$

λ	β	N	n_s	r	V_0	α	ES
1.0	22	85	0.9604	0.0569	6.33×10^{-10}	3.10×10^{-6}	4.92×10^{-3}
1.0	22	87	0.9609	0.0534	5.91×10^{-10}	2.99×10^{-6}	4.84×10^{-3}
1.0	23	85	0.9609	0.0616	6.92×10^{-10}	3.17×10^{-6}	5.02×10^{-3}
1.0	23	87	0.9615	0.0579	6.46×10^{-10}	3.06×10^{-6}	4.94×10^{-3}
10^2	22	85	0.9605	0.0568	9.43×10^{-12}	2.69×10^{-6}	1.72×10^{-3}
10^2	22	87	0.9611	0.0533	8.80×10^{-12}	2.59×10^{-6}	1.69×10^{-3}
10^2	23	85	0.9610	0.0615	1.03×10^{-11}	2.75×10^{-6}	1.75×10^{-3}
10^2	23	87	0.9616	0.0577	9.63×10^{-12}	2.65×10^{-6}	1.73×10^{-3}
10^4	22	85	0.9605	0.0568	9.48×10^{-14}	2.68×10^{-6}	5.44×10^{-4}
10^4	22	87	0.9611	0.0532	8.84×10^{-14}	2.59×10^{-6}	5.36×10^{-4}
10^4	23	85	0.9610	0.0615	1.04×10^{-13}	2.74×10^{-6}	5.55×10^{-4}
10^4	23	87	0.9617	0.0577	9.68×10^{-14}	2.65×10^{-6}	5.47×10^{-4}

TABLE II. The table shows the results of the model for different values of β and λ for the number of e-folds N .

where α and V_0 are two constants that will be determined later. Substituting the potential in Eqs.(17) and (19), the first and second slow-roll parameters are obtained as

$$\epsilon_1 = \frac{3\alpha^2}{2\kappa^2(1+\lambda)V_0} \frac{\sinh^2(\alpha\phi)}{\cosh(\alpha\phi)}, \quad (44)$$

$$\epsilon_2 = \frac{\alpha^2}{\kappa^2(1+\lambda)V_0} \frac{\cosh^2(\alpha\phi) + 1}{\cosh(\alpha\phi)}, \quad (45)$$

and from Eq.(16), the time derivative of the tachyon field is

$$\dot{\phi}^2 = \frac{\alpha^2(1+2\lambda)}{\kappa^2(1+\lambda)^2V_0} \frac{\sinh^2(\alpha\phi)}{\cosh(\alpha\phi)}. \quad (46)$$

To estimate the parameters at the time of the horizon crossing, we first need to compute the field at the end of inflation. It is done by solving the relation $\epsilon_1 = 1$ that implies the time when the universe acceleration vanishes. It leads to

$$\sinh(\alpha\phi_e) = \frac{\beta^2}{2} \left(1 + \sqrt{1 + \frac{4}{\beta^2}} \right), \quad (47)$$

where the constant β is defined for more simplicity and is read as

$$\beta \equiv \frac{2\kappa^2(1+\lambda)V_0}{3\alpha^2}. \quad (48)$$

Then, through the number of e-folds relation and using the above result, the field is read during inflation as

$$\tanh\left(\frac{\alpha\phi_\star}{2}\right) = \tanh\left(\frac{\alpha\phi_e}{2}\right) \exp\left(\frac{-2}{3\beta} N\right). \quad (49)$$

Applying the above tachyon field on the equations

$$n_s = 1 - \frac{2}{3\beta} \frac{2\sinh^2(\alpha\phi_\star) + 1}{\cosh(\alpha\phi_\star)}, \quad (50)$$

$$r = \frac{16}{\beta} \frac{\sinh^2(\alpha\phi_\star)}{\cosh(\alpha\phi_\star)}. \quad (51)$$

the scalar spectral index and the tensor-to-scalar ratio are determined at the time of the horizon crossing in terms of the two parameters β and the number of e-folds N . The behavior of the $r - n_s$ curves in terms of β and for different time of the horizon crossing are depicted in Fig.5. It is found that the curves with higher number of e-folds stand better in the observational range and describe a more suitable consistency with the data. One could also determine the proper values of β and N in order to establish a consistency between the model and data by creating a Python coding and imposing data on it. The result will be a parametric space of β and N , presented in Fig.6, so that for

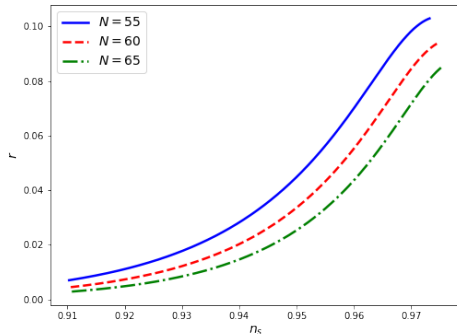


FIG. 5. The figure illustrates the $r - n_s$ curves in terms of β and for different values of the number of e-folds.

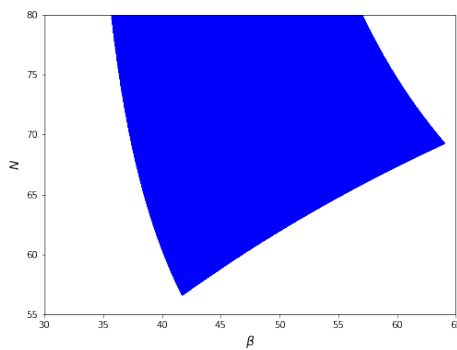


FIG. 6. The figure shows the parameter space of β and N for which for every point in this space the model provides the scalar spectral index and the tensor-to-scalar ratio standing the observational range.

every (β, N) point in the space the model comes to an agreement with data. Another observational parameter which there is an exact data for it is the amplitude of the scalar perturbations. The parameter is given by Eq.(20) in the model. Using the Friedmann equation (13), the defined potential, and by computing the equation at the time of the horizon crossing, one could estimate a valid value for the constant V_0 of the model as

$$V_0 = \frac{24\pi^2}{\kappa^2(1+2\lambda)} c_s \epsilon_1 \mathcal{P}_s^* \cosh(\alpha\phi_*). \quad (52)$$

A brief result of the model is presented in Table.III, where one could find the values for the scalar spectral index, the tensor-to-scalar ratio, the constant V_0 , and the energy scale of inflation for different values of β and N selected from Fig.6.

V. CONCLUSION

In this study, we investigated the scenario of tachyon inflation within the framework of the modified theory of $f(R, T)$ gravity. This theory includes a non-minimal inflaton-curvature coupling, which arises from including the trace of the energy-momentum tensor in the action. To simplify the main dynamical equations of the model, we substituted the energy density and pressure of the tachyon field and applied slow-roll approximations. We then explored the scenario further by introducing three different types of potentials: power-law, generalized T-mode, and inverse hyperbolic cosh. Using Python coding and observational data, we determined the range of values for the free parameters of the model that allowed it to fit the data.

For the power-law potential, we found that preserving agreement with the data required a positive power value less than 0.28 and a maximum number of e-folds of 47, which is lower than the desired value of 60. The estimated energy scale of inflation was of the order of $\mathcal{O}(10^{-3})$; lower than the Planck scale.

λ	β	N	n_s	r	V_0	α	ES
1.0	45	60	0.9626	0.0626	7.05×10^{-10}	4.57×10^{-6}	5.04×10^{-3}
1.0	45	65	0.9638	0.0533	5.93×10^{-10}	4.19×10^{-6}	4.84×10^{-3}
1.0	50	60	0.9647	0.0689	7.92×10^{-10}	4.59×10^{-6}	5.16×10^{-3}
1.0	50	65	0.9659	0.0595	6.73×10^{-10}	4.24×10^{-6}	4.98×10^{-3}
10^2	45	60	0.9627	0.0625	1.05×10^{-11}	3.96×10^{-6}	1.76×10^{-3}
10^2	45	65	0.9639	0.0532	8.83×10^{-12}	3.63×10^{-6}	1.69×10^{-3}
10^2	50	60	0.9648	0.0687	1.18×10^{-11}	3.98×10^{-6}	1.80×10^{-3}
10^2	50	65	0.9660	0.0593	1.00×10^{-11}	3.67×10^{-6}	1.74×10^{-3}
10^4	45	60	0.9627	0.0625	1.06×10^{-13}	3.95×10^{-6}	5.58×10^{-4}
10^4	45	65	0.9639	0.0532	8.87×10^{-14}	3.63×10^{-6}	5.36×10^{-4}
10^4	50	60	0.9648	0.0687	1.18×10^{-13}	3.97×10^{-6}	5.71×10^{-4}
10^4	50	65	0.9660	0.0593	1.01×10^{-13}	3.66×10^{-6}	5.50×10^{-4}

TABLE III. The table present a brief results of the case for different values of β and λ for the number of e-folds N .

In the case of the generalized T-mode potential, the model agreed with the data for a number of e-folds larger than 80, but only for a narrow range of the parameter β . The range became wider for larger values of the number of e-folds, but these larger values were outside of our scope of interest.

Finally, for the inverse hyperbolic cosh potential, we determined the suitable range for the parameters β and the number of e-folds through performing a Python coding. As the number of e-folds increased towards 70, the valid range of β also became wider. The estimated energy scale of inflation for the obtained free parameters was of the order of $\mathcal{O}(10^{-3})M_p$, similar to the previous cases. The advantage of this case compared to the others was that the model was able to fit the data for a proper value of the number of e-folds.

Overall, this study provides new insights into the scenario of tachyon inflation within the $f(R, T)$ gravity theory, highlighting its potential as a useful alternative framework.

-
- [1] A. A. Starobinsky, A new type of isotropic cosmological models without singularity, *Physics Letters B* **91**, 99 (1980).
- [2] A. H. Guth, The Inflationary Universe: A Possible Solution to the Horizon and Flatness Problems, *Phys. Rev.* **D23**, 347 (1981), [Adv. Ser. Astrophys. Cosmol.3,139(1987)].
- [3] A. Albrecht and P. J. Steinhardt, Cosmology for grand unified theories with radiatively induced symmetry breaking, *Physical Review Letters* **48**, 1220 (1982).
- [4] A. D. Linde, A new inflationary universe scenario: a possible solution of the horizon, flatness, homogeneity, isotropy and primordial monopole problems, *Physics Letters B* **108**, 389 (1982).
- [5] A. D. Linde, Chaotic inflation, *Physics Letters B* **129**, 177 (1983).
- [6] G. Barenboim and W. H. Kinney, Slow roll in simple non-canonical inflation, *JCAP* **0703**, 014, arXiv:astro-ph/0701343 [astro-ph].
- [7] P. Franche, R. Gwyn, B. Underwood, and A. Wissanji, Initial Conditions for Non-Canonical Inflation, *Phys. Rev.* **D82**, 063528 (2010), arXiv:1002.2639 [hep-th].
- [8] S. Unnikrishnan, V. Sahni, and A. Toporensky, Refining inflation using non-canonical scalars, *JCAP* **1208**, 018, arXiv:1205.0786 [astro-ph.CO].
- [9] K. Rezazadeh, K. Karami, and P. Karimi, Intermediate inflation from a non-canonical scalar field, *JCAP* **1509** (09), 053, arXiv:1411.7302 [gr-qc].
- [10] K. Saaidi, A. Mohammadi, and T. Golanbari, Light of Planck-2015 on Noncanonical Inflation, *Adv. High Energy Phys.* **2015**, 926807 (2015), arXiv:1708.03675 [gr-qc].
- [11] M. Fairbairn and M. H. G. Tytgat, Inflation from a tachyon fluid?, *Phys. Lett.* **B546**, 1 (2002), arXiv:hep-th/0204070 [hep-th].
- [12] S. Mukohyama, Brane cosmology driven by the rolling tachyon, *Phys. Rev.* **D66**, 024009 (2002), arXiv:hep-th/0204084 [hep-th].
- [13] A. Feinstein, Power law inflation from the rolling tachyon, *Phys. Rev.* **D66**, 063511 (2002), arXiv:hep-th/0204140 [hep-th].
- [14] T. Padmanabhan, Accelerated expansion of the universe driven by tachyonic matter, *Phys. Rev.* **D66**, 021301 (2002), arXiv:hep-th/0204150 [hep-th].
- [15] A. Aghamohammadi, A. Mohammadi, T. Golanbari, and K. Saaidi, Hamilton-Jacobi formalism for tachyon inflation, *Phys. Rev.* **D90**, 084028 (2014), arXiv:1502.07578 [gr-qc].
- [16] M. Spalinski, On Power law inflation in DBI models, *JCAP* **0705**, 017, arXiv:hep-th/0702196 [hep-th].
- [17] D. Bessada, W. H. Kinney, and K. Tzirakis, Inflationary potentials in DBI models, *JCAP* **0909**, 031, arXiv:0907.1311 [gr-qc].

- [18] J. M. Weller, C. van de Bruck, and D. F. Mota, Inflationary predictions in scalar-tensor DBI inflation, *JCAP* **1206**, 002, arXiv:1111.0237 [astro-ph.CO].
- [19] N. Nazavari, A. Mohammadi, Z. Ossoulian, and K. Saaidi, Intermediate inflation driven by DBI scalar field, *Phys. Rev.* **D93**, 123504 (2016), arXiv:1708.03676 [gr-qc].
- [20] K.-i. Maeda and K. Yamamoto, Stability analysis of inflation with an $su(2)$ gauge field, *Journal of Cosmology and Astroparticle Physics* **2013** (12), 018.
- [21] A. A. Abolhasani, R. Emami, and H. Firouzjahi, Primordial anisotropies in gauged hybrid inflation, *Journal of Cosmology and Astroparticle Physics* **2014** (05), 016.
- [22] S. Alexander, D. Jyoti, A. Kosowsky, and A. Marcianò, Dynamics of gauge field inflation, *Journal of Cosmology and Astroparticle Physics* **2015** (05), 005.
- [23] M. Tirandari, K. Saaidi, and A. Mohammadi, Anisotropic inflation in brans-dicke gravity with a non-abelian gauge field, *Phys. Rev. D* **98**, 043516 (2018).
- [24] R. Maartens, D. Wands, B. A. Bassett, and I. P. Heard, Chaotic inflation on the brane, *Physical Review D* **62**, 041301 (2000).
- [25] T. Golanbari, A. Mohammadi, and K. Saaidi, Brane inflation driven by noncanonical scalar field, *Physical Review D* **89**, 103529 (2014).
- [26] A. Mohammadi, T. Golanbari, S. Nasri, and K. Saaidi, Brane inflation: Swampland criteria, TCC, and reheating predictions, *Astropart. Phys.* **142**, 102734 (2022), arXiv:2006.09489 [gr-qc].
- [27] A. Mohammadi, T. Golanbari, and J. Enayati, Brane inflation and trans-Planckian censorship conjecture, *Phys. Rev. D* **104**, 123515 (2021), arXiv:2012.01512 [hep-th].
- [28] A. Mohammadi, A. F. Ali, T. Golanbari, A. Aghamohammadi, K. Saaidi, and M. Faizal, Inflationary universe in the presence of a minimal measurable length, *Annals Phys.* **385**, 214 (2017), arXiv:1505.04392 [gr-qc].
- [29] A. Mohammadi, Z. Ossoulian, T. Golanbari, and K. Saaidi, Intermediate inflation with modified kinetic term, *Astrophys. Space Sci.* **359**, 7 (2015).
- [30] A. Berera, Warm inflation, *Physical Review Letters* **75**, 3218 (1995).
- [31] A. Berera, Warm inflation in the adiabatic regime—a model, an existence proof for inflationary dynamics in quantum field theory, *Nuclear Physics B* **585**, 666 (2000).
- [32] L. M. Hall, I. G. Moss, and A. Berera, Scalar perturbation spectra from warm inflation, *Physical Review D* **69**, 083525 (2004).
- [33] K. Sayar, A. Mohammadi, L. Akhtari, and K. Saaidi, Hamilton-Jacobi formalism to warm inflationary scenario, *Phys. Rev.* **D95**, 023501 (2017), arXiv:1708.01714 [gr-qc].
- [34] L. Akhtari, A. Mohammadi, K. Sayar, and K. Saaidi, Viscous warm inflation: Hamilton–Jacobi formalism, *Astropart. Phys.* **90**, 28 (2017), arXiv:1710.05793 [astro-ph.CO].
- [35] H. Sheikahmadi, A. Mohammadi, A. Aghamohammadi, T. Harko, R. Herrera, C. Corda, A. Abebe, and K. Saaidi, Constraining chameleon field driven warm inflation with Planck 2018 data, *Eur. Phys. J.* **C79**, 1038 (2019), arXiv:1907.10966 [gr-qc].
- [36] A. Mohammadi, T. Golanbari, H. Sheikahmadi, K. Sayar, L. Akhtari, M. Rasheed, and K. Saaidi, Warm tachyon inflation and swampland criteria, *Chin. Phys. C* **44**, 095101 (2020), arXiv:2001.10042 [gr-qc].
- [37] A. Mohammadi, K. Saaidi, and T. Golanbari, Tachyon constant-roll inflation, *Phys. Rev.* **D97**, 083006 (2018), arXiv:1801.03487 [hep-ph].
- [38] A. Mohammadi, K. Saaidi, and H. Sheikahmadi, Constant-roll approach to non-canonical inflation, *Phys. Rev.* **D100**, 083520 (2019), arXiv:1803.01715 [astro-ph.CO].
- [39] T. Golanbari, A. Mohammadi, and K. Saaidi, Observational constraints on DBI constant-roll inflation, *Phys. Dark Univ.* **27**, 100456 (2020), arXiv:1808.07246 [gr-qc].
- [40] A. Mohammadi, T. Golanbari, and K. Saaidi, Beta-function formalism for k-essence constant-roll inflation, *Phys. Dark Univ.* **28**, 100505 (2020), arXiv:1912.07006 [gr-qc].
- [41] A. Mohammadi, T. Golanbari, S. Nasri, and K. Saaidi, Constant-roll brane inflation, *Phys. Rev. D* **101**, 123537 (2020), arXiv:2004.12137 [gr-qc].
- [42] A. Mohammadi, T. Golanbari, K. Bamba, and I. P. Lobo, Tsallis holographic dark energy for inflation, *Phys. Rev. D* **103**, 083505 (2021), arXiv:2101.06378 [gr-qc].
- [43] A. Mohammadi, Holographic warm inflation, *Phys. Rev. D* **104**, 123538 (2021), arXiv:2109.00247 [gr-qc].
- [44] A. Mohammadi, Constant-roll inflation driven by holographic dark energy, *Phys. Dark Univ.* **36**, 101055 (2022), arXiv:2203.06643 [gr-qc].
- [45] A. Mohammadi, T. Golanbari, J. Enayati, S. Jalalzadeh, S. Nasri, and K. Saaidi, Swampland criteria and reheating predictions in scalar–tensor inflation, *Int. J. Mod. Phys. D* **31**, 2250079 (2022).
- [46] A. D. Linde, Inflationary cosmology, *Phys. Rept.* **333**, 575 (2000).
- [47] A. D. Linde, Particle physics and inflationary cosmology, *Contemp. Concepts Phys.* **5**, 1 (1990), arXiv:hep-th/0503203 [hep-th].
- [48] A. D. Linde, Current understanding of inflation, *Proceedings, 6th UCLA Symposium on Sources and Detection of Dark Matter and Dark Energy in the Universe: Marina del Rey, CA, USA, February 18-20, 2004*, *New Astron. Rev.* **49**, 35 (2005).
- [49] A. D. Linde, Prospects of inflation, *Proceedings, Nobel Symposium 127 on String theory and cosmology: Sigtuna, Sweden, August 14-19, 2003*, *Phys. Scripta* **T117**, 40 (2005), arXiv:hep-th/0402051 [hep-th].

- [50] A. Riotto, Inflation and the theory of cosmological perturbations, *Astroparticle physics and cosmology. Proceedings: Summer School, Trieste, Italy, Jun 17-Jul 5 2002*, ICTP Lect. Notes Ser. **14**, 317 (2003), arXiv:hep-ph/0210162 [hep-ph].
- [51] D. Baumann, TASI Lecture on Inflation, in *Physics of the large and the small, TASI 09, proceedings of the Theoretical Advanced Study Institute in Elementary Particle Physics, Boulder, Colorado, USA, 1-26 June 2009* (2011) pp. 523–686, arXiv:0907.5424 [hep-th].
- [52] S. Weinberg, *Cosmology* (2008).
- [53] D. H. Lyth and A. R. Liddle, *The primordial density perturbation: Cosmology, inflation and the origin of structure* (2009).
- [54] A. R. Liddle and D. H. Lyth, *Cosmological inflation and large scale structure* (2000).
- [55] P. A. R. Ade *et al.* (Planck), Planck 2013 results. XXII. Constraints on inflation, *Astron. Astrophys.* **571**, A22 (2014), arXiv:arXiv:1303.5082 [astro-ph.CO].
- [56] P. A. R. Ade *et al.* (Planck), Planck 2015 results. XX. Constraints on inflation, *Astron. Astrophys.* **594**, A20 (2016), arXiv:arXiv:1502.02114 [astro-ph.CO].
- [57] Y. Akrami *et al.* (Planck), Planck 2018 results. X. Constraints on inflation, (2018), arXiv:arXiv:1807.06211 [astro-ph.CO].
- [58] T. Golanbari, T. Haddad, A. Mohammadi, M. A. Rasheed, and K. Saaidi, Quark-hadron phase transition in DGP including BD brane, *Chin. Phys. C* **44**, 083109 (2020), arXiv:1401.5029 [gr-qc].
- [59] T. Golanbari, A. Mohammadi, Z. Ossoulian, and K. Saaidi, Quark-Hadron Phase Transition in DGP Brane Gravity with Bulk Scalar Field, *Astrophys. Space Sci.* **357**, 159 (2015), arXiv:1404.2142 [hep-th].
- [60] T. Golanbari, A. Mohammadi, and K. Saaidi, QCD phase transition with a power law chameleon scalar field in the bulk, *Int. J. Mod. Phys. A* **29**, 1450033 (2014), arXiv:1401.4906 [gr-qc].
- [61] A. Aghamohammadi, K. Saaidi, A. Mohammadi, H. Sheikahmadi, T. Golanbari, and S. W. Rabiei, Effect of an external interaction mechanism in solving agegraphic dark energy problems, *Astrophys. Space Sci.* **345**, 17 (2013), arXiv:1402.2608 [physics.gen-ph].
- [62] 10.1103/physrevd.86.045007.
- [63] K. Saaidi and A. Mohammadi, Brane Cosmology with the Chameleon Scalar Field in Bulk, *Phys. Rev. D* **85**, 023526 (2012), arXiv:1201.0371 [gr-qc].
- [64] K. Saaidi, H. Sheikahmadi, and A. H. Mohammadi, Interacting New Agegraphic Dark Energy in a Cyclic Universe, *Astrophys. Space Sci.* **338**, 355 (2012), arXiv:1201.0275 [gr-qc].
- [65] K. Saaidi, A. Mohammadi, and H. Sheikahmadi, γ Parameter and Solar System constraint in Chameleon Brans Dick theory, *Phys. Rev. D* **83**, 104019 (2011), arXiv:1201.0271 [gr-qc].
- [66] K. Saaidi and A. H. Mohammadi, Brane Cosmology With Generalized Chaplygin Gas in The Bulk, *Mod. Phys. Lett. A* **25**, 3061 (2010), arXiv:1006.1847 [gr-qc].
- [67] T. Harko, F. S. N. Lobo, S. Nojiri, and S. D. Odintsov, $f(R, T)$ gravity, *Phys. Rev. D* **84**, 024020 (2011), arXiv:1104.2669 [gr-qc].
- [68] J. a. L. Rosa and P. M. Kull, Non-exotic traversable wormhole solutions in linear $f(R, T)$ gravity, *Eur. Phys. J. C* **82**, 1154 (2022), arXiv:2209.12701 [gr-qc].
- [69] T. B. Gonçalves, J. a. L. Rosa, and F. S. N. Lobo, Cosmological sudden singularities in $f(R, T)$ gravity, *Eur. Phys. J. C* **82**, 418 (2022), arXiv:2203.11124 [gr-qc].
- [70] T. B. Gonçalves, J. a. L. Rosa, and F. S. N. Lobo, Cosmology in scalar-tensor $f(R, T)$ gravity, *Phys. Rev. D* **105**, 064019 (2022), arXiv:2112.02541 [gr-qc].
- [71] J. a. L. Rosa, Junction conditions and thin shells in perfect-fluid $f(R, T)$ gravity, *Phys. Rev. D* **103**, 104069 (2021), arXiv:2103.11698 [gr-qc].
- [72] M. Z.-U.-H. Bhatti and Z. Yousaf, Dynamical variables and evolution of the universe, *Int. J. Mod. Phys. D* **26**, 1750029 (2016).
- [73] R. Zaregonbadi, M. Farhoudi, and N. Riazi, Dark Matter From $f(R, T)$ Gravity, *Phys. Rev. D* **94**, 084052 (2016), arXiv:1608.00469 [gr-qc].
- [74] P. H. R. S. Moraes and P. K. Sahoo, Wormholes in exponential $f(R, T)$ gravity, *Eur. Phys. J. C* **79**, 677 (2019), arXiv:1903.03421 [gr-qc].
- [75] M. E. S. Alves, P. H. R. S. Moraes, J. C. N. de Araujo, and M. Malheiro, Gravitational waves in $f(R, T)$ and $f(R, T^\phi)$ theories of gravity, *Phys. Rev. D* **94**, 024032 (2016), arXiv:1604.03874 [gr-qc].
- [76] S. Bhattacharjee, J. R. L. Santos, P. H. R. S. Moraes, and P. K. Sahoo, Inflation in $f(R, T)$ gravity, *Eur. Phys. J. Plus* **135**, 576 (2020), arXiv:2006.04336 [gr-qc].
- [77] M. Gamonal, Slow-roll inflation in $f(R, T)$ gravity and a modified Starobinsky-like inflationary model, *Phys. Dark Univ.* **31**, 100768 (2021), arXiv:2010.03861 [gr-qc].
- [78] S. Taghavi, K. Saaidi, Z. Ossoulian, and T. Golanbari, Holographic inflation in $f(R, T)$ gravity, (2023), arXiv:2301.02631 [gr-qc].
- [79] Z. Ossoulian, K. Saaidi, S. Taghavi, and T. Golanbari, Noncanonical inflation in $f(R, T)$ gravity with Hamilton-Jacobi formalism, (2023), arXiv:2301.08319 [gr-qc].
- [80] S. Choudhury and S. Panda, COSMOS-e'-GTachyon from string theory, *Eur. Phys. J. C* **76**, 278 (2016), arXiv:1511.05734 [hep-th].
- [81] P. H. R. S. Moraes, J. D. V. Arbañil, and M. Malheiro, Stellar equilibrium configurations of compact stars in $f(R, T)$ gravity, *JCAP* **06**, 005, arXiv:1511.06282 [gr-qc].
- [82] G. A. Carvalho, R. V. Lobato, P. H. R. S. Moraes, J. D. V. Arbañil, R. M. Marinho, E. Otoniel, and M. Malheiro, Stellar equilibrium configurations of white dwarfs in the $f(R, T)$ gravity, *Eur. Phys. J. C* **77**, 871 (2017), arXiv:1706.03596 [gr-qc].

- [83] P. H. R. S. Moraes, W. de Paula, and R. A. C. Correa, Charged wormholes in $f(R,T)$ extended theory of gravity, *Int. J. Mod. Phys. D* **28**, 1950098 (2019), arXiv:1710.07680 [gr-qc].
- [84] P. H. R. S. Moraes and P. K. Sahoo, Modelling wormholes in $f(R,T)$ gravity, *Phys. Rev. D* **96**, 044038 (2017), arXiv:1707.06968 [gr-qc].
- [85] P. H. R. S. Moraes, R. A. C. Correa, and R. V. Lobato, Analytical general solutions for static wormholes in $f(R,T)$ gravity, *JCAP* **07**, 029, arXiv:1701.01028 [gr-qc].
- [86] T. Azizi, Wormhole Geometries In $f(R,T)$ Gravity, *Int. J. Theor. Phys.* **52**, 3486 (2013), arXiv:1205.6957 [gr-qc].
- [87] P. H. R. S. Moraes, Cosmology from induced matter model applied to 5D $f(R,T)$ theory, *Astrophys. Space Sci.* **352**, 273 (2014).
- [88] P. H. R. S. Moraes, Cosmological solutions from Induced Matter Model applied to 5D $f(R,T)$ gravity and the shrinking of the extra coordinate, *Eur. Phys. J. C* **75**, 168 (2015), arXiv:1502.02593 [gr-qc].
- [89] D. R. K. Reddy and R. Santhi Kumar, Some anisotropic cosmological models in a modified theory of gravitation, *Astrophys. Space Sci.* **344**, 253 (2013).
- [90] J. Garriga and V. F. Mukhanov, Perturbations in k-inflation, *Phys. Lett.* **B458**, 219 (1999), arXiv:hep-th/9904176 [hep-th].
- [91] F. Leblond and A. W. Peet, SD brane gravity fields and rolling tachyons, *JHEP* **04**, 048, arXiv:hep-th/0303035.
- [92] C.-j. Kim, H. B. Kim, Y.-b. Kim, and O.-K. Kwon, Electromagnetic string fluid in rolling tachyon, *JHEP* **03**, 008, arXiv:hep-th/0301076.
- [93] A. Maloney, A. Strominger, and X. Yin, S-brane thermodynamics, *JHEP* **10**, 048, arXiv:hep-th/0302146.
- [94] D. A. Steer and F. Vernizzi, Tachyon inflation: Tests and comparison with single scalar field inflation, *Phys. Rev. D* **70**, 043527 (2004), arXiv:hep-th/0310139.